

Influence of preservation temperature on the characteristics of anaerobic ammonium oxidation (anammox) granular sludge

Bao-Shan Xing^{1,2} · Qiong Guo^{1,2} · Xiao-Yan Jiang^{1,2} · Qian-Qian Chen^{1,2} · Peng Li^{1,2} · Wei-Min Ni^{1,2} · Ren-Cun Jin^{1,2}

Received: 28 November 2015 / Revised: 28 December 2015 / Accepted: 30 December 2015 / Published online: 16 January 2016
© Springer-Verlag Berlin Heidelberg 2016

Abstract Preserving active anaerobic ammonium oxidation (anammox) biomass is a potential method for securing sufficient seeding biomass for the rapid start-up of full-scale anammox processes. In this study, anammox granules were cultured in an upflow anaerobic sludge blanket (UASB) reactor (R_0), and then the enriched anammox granules were preserved at 35, 20, 4, and -30 °C. The subsequent reactivation characteristics of the granules were evaluated in four UASB reactors (denoted R_1 , R_2 , R_3 , and R_4 , respectively) to investigate the effect of preservation temperature on the characteristics of anammox granules and their reactivation performance. The results demonstrated that 4 °C was the optimal preservation temperature for maintaining the biomass, activity, settleability, and integrity of the anammox granules and their cellular structures. During the preservation period, a first-order exponential decay model may be used to simulate the decay of anammox biomass and activity. The protein-to-polysaccharide ratio in the extracellular polymeric substances and the heme *c* content could not effectively indicate the changes in settleability and activity of the anammox granules, respectively, and a loss of bioactivity was positively associated with the degree of anaerobic ammonium-oxidizing bacteria

cell lysis. After 42 days of storage, the anammox granules preserved at 4 °C (R_3) exhibited a better recovery performance than those preserved at 20 °C (R_2), -30 °C (R_4), and 35 °C (R_1). The comprehensive comparison indicated that 4 °C is the optimal storage temperature for anammox granular sludge because it promotes improved maintenance and recovery performance properties.

Keywords Anammox · Granular sludge · Preservation temperature · Reactivation · Granule characteristics

Introduction

The anaerobic ammonium oxidation (anammox) process refers to the oxidization of ammonium to nitrogen gas using nitrite as the electron acceptor in the absence of oxygen (Ding et al. 2013). As an innovative and sustainable biological nitrogen-removal alternative to traditional nitrification-denitrification technology, the anammox process has several advantages, including negligible excess sludge production, low energy consumption, and no external organic carbon requirement (van der Star et al. 2007). Applying the anammox process to remove nitrogen from municipal sewage allows for wastewater treatment plant procedures that promote net energy production (Kartal et al. 2010). Energy-positive wastewater treatments have the potential to increase societal sustainability, and anammox is a key process in achieving this goal (Lotti et al. 2015; Xu et al. 2015).

Although the anammox process has many advantages, one of its disadvantages is related to the long system start-up period, which is caused by the slow growth rate of the anammox consortium (typical doubling time of 15–30 days) (Ali and Okabe 2015; Lotti et al. 2015; Strous et al. 1998; van der Star et al. 2007). The start-up of the anammox process was

Electronic supplementary material The online version of this article (doi:10.1007/s00253-016-7292-3) contains supplementary material, which is available to authorized users.

✉ Ren-Cun Jin
jrczju@aliyun.com

¹ College of Life and Environmental Sciences, Hangzhou Normal University, Hangzhou 310036, China

² Key Laboratory of Hangzhou City for Ecosystem Protection and Restoration, Hangzhou Normal University, Hangzhou 310036, China

significantly accelerated in the presence of mature anammox seeds (van der Star et al. 2007; Wett 2006). Sequential biomass additions have been shown to be an effective method for increasing the development and growth of anammox bacteria (Jin et al. 2013a). Adding fresh anammox sludge to the anammox reactor, which is referred to as bioaugmentation, increases the biomass and reduces the unit-sludge loading rate over a short time and may also introduce growth factors that favor regrowth after inhibition (Jin et al. 2012). Additionally, in terms of the working mode, the wastewater flow could be stopped for several weeks or even months because of seasonal closure of the industry and annual maintenance or vacation periods, which are common in biological wastewater treatment industries (Leitão et al. 2006). Therefore, the preservation of anammox biomass is an inevitable technical issue when applying the anammox process (Ali et al. 2014).

Anammox granules have several advantages over flocculent sludge, such as a denser and stronger aggregate structure, more likely solid-effluent separation, higher biomass concentration, and greater ability to withstand shock loadings and toxicity. The granule-based process is applied in more than 20 % of all full-scale partial nitrification-anammox systems (Lackner et al. 2014). However, the properties of anammox granules are important factors that affect the performance and robustness of the process. The biomass and specific anammox activity (SAA) together determine the performance of the anammox process. The particle size of the anammox granules affects their mass transfer and settleability, and extracellular polymeric substances (EPS) influence the stress tolerance of the granules (Xing et al. 2015). Therefore, it is essential to track the sludge characteristics and reactivation performance of the anammox process during preservation.

Temperature is a key condition for bacteria preservation. High temperatures are not conducive to long-term microbial storage because of the high microbial decay rate without an adequate supply of substrates. However, the structure of anaerobic ammonium-oxidizing bacteria cells may be destroyed under low temperatures. Therefore, the storage temperature must be optimized for the development and utilization of microbial resources.

Previous studies have investigated the storage of anammox bacteria under different temperatures (e.g., -200 , -20 , and 4 °C). In one study, the anammox activity of oxygen-limited autotrophic nitrification/denitrification (OLAND) biomass was lost after 2 months of storage at -20 °C (Vlaeminck et al. 2007), whereas in another study, pre-freezing with liquid nitrogen (-200 °C) was required for the long-term preservation of anammox bacteria via lyophilization (Rothrock et al. 2011). Moreover, Ji and Jin (2014) studied the impact of preservation conditions (at 4 °C) on the reactivation performance of an anammox reactor. Furthermore, a moderate temperature of 36 °C was also been investigated for the preservation of anammox granular sludge (Wu et al. 2015). However, few

systemic studies have been performed to determine the impacts of storage temperature on the properties of anammox granular sludge.

Therefore, the goal of this study is to determine the optimal preservation temperature for the storage of anammox granular sludge over a long period and the subsequent reactivation of the system. In this study, we investigated the effects of storage for up to 6 weeks under different preservation temperatures (35 , 20 , 4 , and -30 °C) on the properties of anammox granules (e.g., SAA, granule diameter, sludge settling properties, EPS, heme *c* content, and granular sludge morphology). The subsequent reactivation performance and properties of the anammox granules were also investigated.

Materials and methods

Synthetic wastewater, anammox granule origins, and operation strategies

To prepare the synthetic wastewater, ammonium and nitrite were added to the mineral medium at a molar ratio of 1:1 in the forms of $(\text{NH}_4)_2\text{SO}_4$ and NaNO_2 , respectively. The composition of the synthetic wastewater was reported in Jin et al. (2013b). Anammox granular sludge for seed sludge was collected from a 2.8-L laboratory-scale anammox upflow anaerobic sludge blanket (UASB) reactor as reported by Xing et al. (2014). This bioreactor, hereafter called the parent bioreactor (R_0), was operated in a thermostatic room at 35 ± 1 °C. The bioreactor sampled was operated in a laboratory site in Hangzhou ($30^\circ 15$ N, $120^\circ 10$ E). Hangzhou is located in northwestern Zhejiang province in the south-central portion of the Yangtze River Delta in southeast China. The R_0 was continuously operated for approximately 2 months. During this period (period A: days 1–65), the nitrogen loading rate (NLR) was increased from 2.23 to $6.39 \text{ kg N m}^{-3} \text{ day}^{-1}$ by adjusting the hydraulic retention time (HRT) and influent nitrogen concentration (TN_{inf}). During the subsequent preservation period (period B: days 65–109), four 1.0-L ground-glass stoppered flasks were applied and each vial was inoculated with 800 mL of $25.89 \text{ g VSS L}^{-1}$ anammox granular sludge. Four vials were emptied with argon in 5–10 min, sealed with Vaseline to maintain the anaerobic conditions, covered with black cloth to avoid light interaction, and then placed in thermostat incubators at 35 , 20 , 4 , and -30 °C. The anammox granules of the four vials were sampled every 2 weeks to determine the properties of the granules (e.g., SAA, granule diameter, sludge settling properties, EPS, heme *c* content, and granular sludge morphology). The anammox granules stored at -30 °C were removed and thawed in a 35 °C water bath for 1 h to measure the granule properties. The applied

temperature and procedure of the measurement of the granules stored at other temperatures were consistent and carried out simultaneously. During the reactivation period (period C: days 109–129), approximately 73 % of the preserved sludge by volume was transferred into four identical 500 mL (working volume) UASB reactors (denoted R₁, R₂, R₃, and R₄ for the sludge preserved at 35, 20, 4, and –30 °C, respectively). The four bioreactors were recovered by feeding relatively low TN_{inf} (140 mg N L⁻¹) and HRTs of 3.0 h in a thermostatic room at 35 ± 1 °C. Then, the TN_{inf} was increased in steps of 28 mg L⁻¹ when the effluent nitrite concentrations were lower than 5 mg L⁻¹ and the 3-day average deviation was less than 10 %. During period C, the SS and sulfide concentration in the effluent were measured every 2 days, and granule samples were collected to measure the granule characteristics when the nitrogen removal performance recovered to its original level. The detailed experimental conditions are shown in Table 1. Vials A, B, C, and D include different treatments that were used for R₁, R₂, R₃, and R₄, respectively.

First-order exponential decay model

The decay rate of the biomass during the starvation phase (period B) was determined by fitting an exponential function to the measured biomass as a function of time (Eq. (1)) (Scaglione et al. 2009; Zhang et al. 2015):

$$Y = A_0 e^{(-b_{AN} \cdot t)} \quad (1)$$

where Y is the remaining biomass (i.e., VSS) as a percentage of the starting value (%), A_0 is a constant, b_{AN} is the decay rate

(day⁻¹), and t is the starvation time (day). From the exponential decay (Eq. (1)), we can define the half-life time (t_{HL}) as follows:

$$t_{HL} = \frac{\ln 2}{b_{AN}}. \quad (2)$$

Analytical methods

The influent and effluent samples were routinely collected and either analyzed immediately or stored in a refrigerator at 4 °C until the analyses were conducted. The SS, VSS, NH₄⁺-N, NO₂⁻-N, and NO₃⁻-N were measured according to standard methods (APHA 2005). The sulfide (S²⁻) concentration was determined using flow injection analysis (FIA) and the spectrophotometric method (AutoAnalyzer 3; Norderstedt, Germany). The pH and temperature were determined using a pH meter (Mettler Toledo Delta 320, Switzerland) and a mercury thermometer, respectively. The SAA assays and granule diameter measurements were performed according to the methods described by Xing et al. (2015). EPS extraction was performed using the “heating” method, and the amounts of carbohydrate and protein in the EPS were estimated as described by Ma et al. (2012). Heme *c* was characterized according to the method described by Berry and Trumpower (1987). The morphological properties of the granules were observed by scanning electron microscopy (SEM) and transmission electron microscopy (TEM) according to the methods described by Xing et al. (2015). Digital imaging was performed using SteREO discovery stereomicroscopes (Nikon SMZ800, Japan) and a digital single-lens reflex camera (Sony NEX-C3, Thailand). The settling velocity was measured by recording

Table 1 Operating conditions and reaction molar ratios in this study

Period	Days	Reactor	HRT (h)	Temp. (°C)	TN_{inf} (mg N L ⁻¹)	Reaction molar ratio	
						R_S^d	R_P^e
A	1–65	R ₀	3.02–1.58	35 ± 1 ^a	280–420 ^b	1.80 ± 0.69	0.29 ± 0.10
B	65–106	Vial A (R ₁)	– ^c	35	–	–	–
		Vial B (R ₂)	–	20	–	–	–
		Vial C (R ₃)	–	4	–	–	–
		Vial D (R ₄)	–	–30	–	–	–
C	106–129	R ₁	3.00	35 ± 1	140–196	0.83 ± 0.43	0.46 ± 0.35
		R ₂	3.00	35 ± 1	140–476	1.43 ± 0.53	0.28 ± 0.16
		R ₃	3.00	35 ± 1	140–532	1.03 ± 0.40	0.13 ± 0.08
		R ₄	3.00	35 ± 1	140–308	1.29 ± 0.28	0.18 ± 0.12

^a Average value ± standard deviation

^b The molar ratio of ammonium to nitrite was 1:1

^c Without nitrogen substrates supplied

^d The ratio of nitrite consumption to ammonium consumption

^e The ratio of nitrate production to ammonium consumption

the time required for the individual granules to fall from a certain height in a measuring cylinder (Jin et al. 2013c). The C, H, and N contents of the granules were measured using an elemental analyzer instrument EA3000 (EuroVector, Italy). The oxygen content was calculated as follows: $O\% = 100\% - (C + H + N)\%$.

Results

Changes in the characteristics of the anammox granular sludge during periods B and C

Biomass and decay kinetics

The seeding sludge in the parent reactor (R_0) was cultured for more than 2 years, and the digital images and optical microscopy images of the anammox granules were published in a previous paper (Xing et al. 2014). The changes in the biomass in the four vials are shown in Table 2. The exponential fitting curves of R_1 – R_4 under different preservation temperatures are provided in Fig. 1. The results indicated that the amount of biomass in the four vials clearly decreased during period B, and the endogenous decay coefficient decreased in the following order: R_1 (35 °C, 0.01726 day^{-1}) > R_2 (20 °C, 0.01346 day^{-1}) > R_3 (4 °C, 0.01228 day^{-1}) > R_4 (–30 °C,

0.00323 day^{-1}). Therefore, the endogenous respiration rate increased as the preservation temperature increased. With an increase of 1 °C for the preservation temperature, the value of the endogenous decay coefficient for the anammox consortium was increased by 0.00021 day^{-1} from the beginning of period B ($R^2 = 0.9732$, Fig. S1). Based on the simulation curve equation (Fig. S1), the endogenous respiration of anammox bacteria can be neglected at preservation temperatures below –48 °C, although this result must be confirmed in a future study. According to Eq. (2), the corresponding t_{HL} values for R_1 , R_2 , R_3 , and R_4 were 40, 51, 56, and 215 days, respectively, which indicated that lower temperatures might be more appropriate for preserving anammox biomass during long-term storage. In addition, the R^2 regression coefficients for R_3 and R_4 were 0.9819 and 0.9201, respectively, indicating that the first-order exponential decay model was more suitable for describing the biomass decay process of anammox granules under lower storage temperature from 4 to –30 °C.

SAA and heme c content

Figure 2a shows the SAA changes in R_1 , R_2 , R_3 , and R_4 during the storage periods under preservation temperatures of 35, 20, 4, and –30 °C, respectively. The bioactivities were decreased during the entire preservation period (days 65–106) of approximately 6 weeks, and the SAA decreased in the order

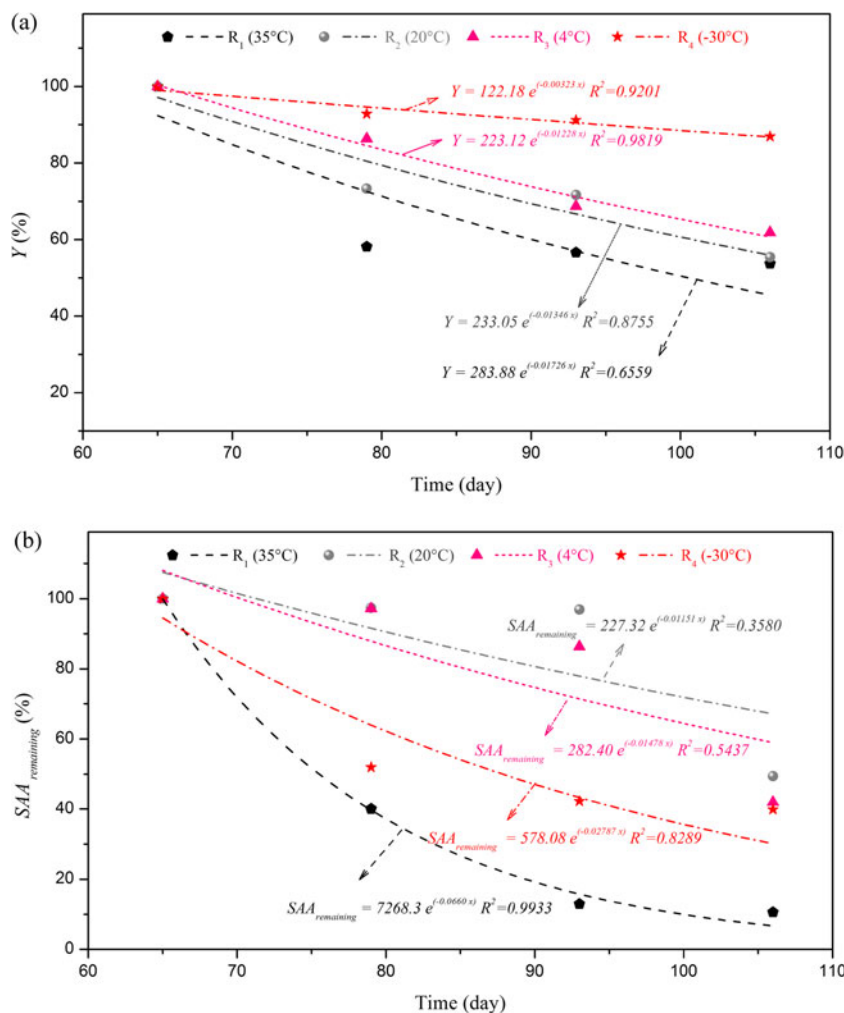
Table 2 Characteristics of the anammox granules under different preservation temperatures during periods B and C

Time (days)	Sludge	SS (g L ⁻¹)	Biomass (g L ⁻¹) ^a	SAA (mg TN g ⁻¹ VSS h ⁻¹) ^b	Heme c content (μmol g ⁻¹ VSS)	Soluble EPS			Bound EPS		
						PS (mg g ⁻¹ VSS)	PN (mg g ⁻¹ VSS)	PN/PS	PS (mg g ⁻¹ VSS)	PN (mg g ⁻¹ VSS)	PN/PS
65	R_0	42.19	25.89	6.72 ± 0.29	3.70 ± 0.04	0.31 ± 0.25	0.51 ± 0.06	2.69 ± 2.09	20.5 ± 0.39	87.4 ± 16.8	4.26 ± 0.74
79	R_1	31.36	15.06	2.69 ± 0.04	8.55 ± 0.14	18.4 ± 24.2	8.19 ± 0.63	1.25 ± 0.94	60.6 ± 1.12	210 ± 33.1	3.48 ± 0.57
	R_2	31.42	18.99	6.54 ± 0.01	7.01 ± 0.13	4.52 ± 0.75	3.74 ± 0.38	0.83 ± 0.08	64.2 ± 8.66	269 ± 15.6	4.24 ± 0.59
	R_3	38.66	22.36	6.53 ± 0.37	3.65 ± 0.02	1.10 ± 0.06	1.33 ± 0.29	1.21 ± 0.24	25.1 ± 1.84	122 ± 4.97	4.88 ± 0.26
	R_4	47.03	24.05	3.49 ± 0.15	4.62 ± 0.06	1.28 ± 0.15	4.51 ± 1.15	3.49 ± 0.55	41.6 ± 0.56	196 ± 25.0	4.72 ± 0.63
93	R_1	34.18	14.66	0.87 ± 0.16	4.96 ± 0.05	4.03 ± 0.42	4.98 ± 0.40	1.24 ± 0.05	35.4 ± 1.13	122 ± 13.3	3.44 ± 0.31
	R_2	32.29	18.56	6.51 ± 0.71	7.76 ± 0.00	6.75 ± 0.43	4.82 ± 1.30	0.71 ± 0.16	48.0 ± 4.24	179 ± 7.84	3.76 ± 0.51
	R_3	28.85	17.80	5.80 ± 0.19	4.25 ± 0.00	3.14 ± 0.45	1.21 ± 1.61	0.35 ± 0.43	26.2 ± 1.15	86.1 ± 14.9	3.30 ± 0.70
	R_4	38.90	23.63	2.84 ± 0.00	4.55 ± 0.07	4.08 ± 0.24	2.51 ± 1.61	0.61 ± 0.37	48.1 ± 2.09	163 ± 3.71	3.39 ± 0.17
106	R_1	30.90	14.60	0.71 ± 0.32	11.7 ± 0.09	2.57 ± 0.81	5.96 ± 0.06	2.46 ± 0.66	47.0 ± 1.82	152 ± 18.3	3.24 ± 0.48
	R_2	33.28	14.34	3.32 ± 0.11	9.77 ± 0.06	1.89 ± 0.29	3.72 ± 0.27	1.99 ± 0.23	51.1 ± 7.02	147 ± 13.2	2.90 ± 0.38
	R_3	32.31	16.01	2.82 ± 0.61	5.08 ± 0.04	1.27 ± 0.14	3.65 ± 0.54	2.94 ± 0.70	29.8 ± 1.26	115 ± 12.9	3.86 ± 0.60
	R_4	39.49	22.51	2.68 ± 0.19	8.93 ± 0.08	1.39 ± 0.57	5.54 ± 0.82	4.26 ± 1.05	86.5 ± 2.82	358 ± 10.0	4.15 ± 0.24
129	R_1	52.03	24.13	0.72 ± 0.11	4.98 ± 0.17	0.71 ± 0.23	2.78 ± 0.52	4.42 ± 2.40	31.7 ± 1.62	138 ± 5.50	4.37 ± 0.13
	R_2	52.76	37.69	3.75 ± 0.05	3.43 ± 0.04	0.91 ± 0.07	3.25 ± 0.48	3.59 ± 0.44	21.7 ± 0.81	92.7 ± 18.8	4.25 ± 0.71
	R_3	57.72	31.91	4.93 ± 0.41	7.31 ± 0.06	1.41 ± 0.21	0.60 ± 0.40	0.41 ± 0.21	26.1 ± 1.38	122 ± 10.4	4.66 ± 0.20
	R_4	51.14	30.28	2.79 ± 0.22	3.04 ± 0.01	0.59 ± 0.10	0.00	0.00	40.0 ± 3.01	194 ± 6.24	4.85 ± 0.24

^a Equal to the value of VSS

^b Average value ± standard deviation.

Fig. 1 Decay kinetic simulation curves of the amount (a) and activity (b) of the anammox granules in R₁, R₂, R₃, and R₄ during the preservation period at different temperature levels (x = t + 64)



$R_2 > R_3 > R_4 > R_1$. For R_1 and R_4 , the SAAs initially decreased rapidly but decreased slightly after storage for approximately 4 weeks, whereas in R_2 and R_3 , the SAAs initially decreased slowly, although this decrease slowed rapidly after storage for approximately 4 weeks. The process that reduces the specific activity of biomass was a key factor in the degree of cell decay, although it was not responsible for reducing the biomass weight. The first-order exponential decay model was also suitable for describing the SAA decay of R_1 and R_4 , and the corresponding modeling equations are as follows:

$$SAA_{remaining} = 7268.3e^{(-0.0660t-4.224)}, R^2 = 0.9933 \quad (3)$$

$$SAA_{remaining} = 578.08e^{(-0.02787t-1.784)}, R^2 = 0.8289 \quad (4)$$

where $SAA_{remaining}$ is the remaining SAA as a percentage of the starting value (%). The b_{AN} rates of the SAA decay in R_1 and R_4 were 0.0660 and 0.02787 day^{-1} , respectively. According to Eq. (2), the half-life time (t_{HL}) of SAA decay in R_4 was 26 days, which is lower than the t_{HL} value (215 days) during the biomass decay process. Therefore, the apparent activity decay was notably greater than the biomass decay in R_4 . In

addition, the SAA and biomass together determine the nitrogen removal potential rates (NRR_{max}). As shown in Fig. 2b, the nitrogen removal capacities in the four vials were different with increased storage time. After approximately 23 days of storage (from 64 to 87 days), the NRR_{max} decreased in the order $R_3 > R_2 > R_4 > R_1$. During a storage time of approximately 23–40 days, the NRR_{max} of R_2 was better than that of R_3 . As the storage time increased to more than 40 days, the freezing temperature of -30°C became the optimal preservation temperature for maintaining the nitrogen removal capacity.

Heme *c* is a cofactor of cytochrome enzymes and peroxidase, and it is widely present in the metabolism of anammox bacteria. Figure 2c shows the changes in heme *c* content within the particles from the four vials. The heme *c* contents of the anammox granules from the four vials have different increments compared with the initial values, which is inconsistent with the change tendency of the SAA during period B (Fig. 2). Therefore, the heme *c* content cannot be used to evaluate the activity of anammox granular sludge during the storage period. This different trend may have been caused by the production of hydrogen sulfide by the anaerobic fermentation of

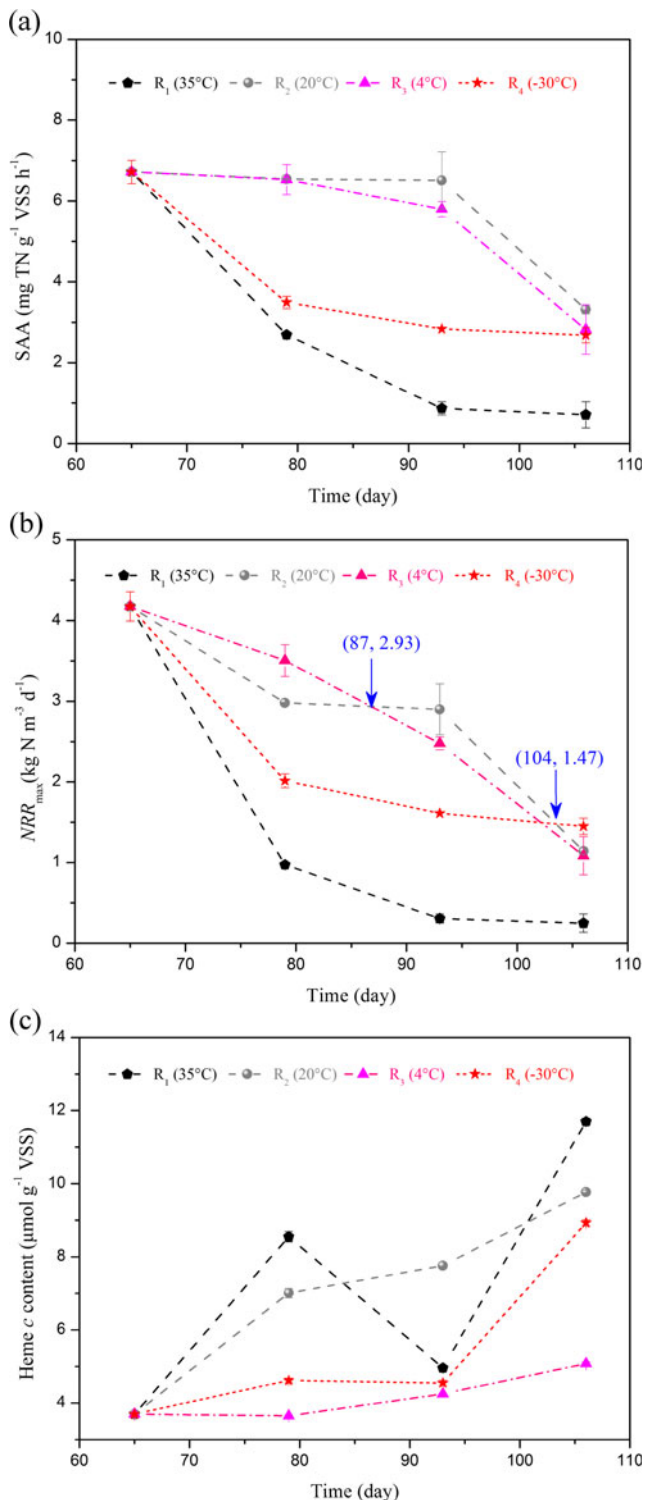


Fig. 2 Variations in the SAA (a), nitrogen removal potential rates (NRR_{max}) (b), and heme c content (c) of the anammox granules from R₁–R₄ during the preservation period at different temperatures

granules during long-term storage. To confirm this assumption, the effluent sulfide concentrations of the four reactors during the reactivation period were measured every 2 days, and the results are listed in Table S1. As expected, the sulfide

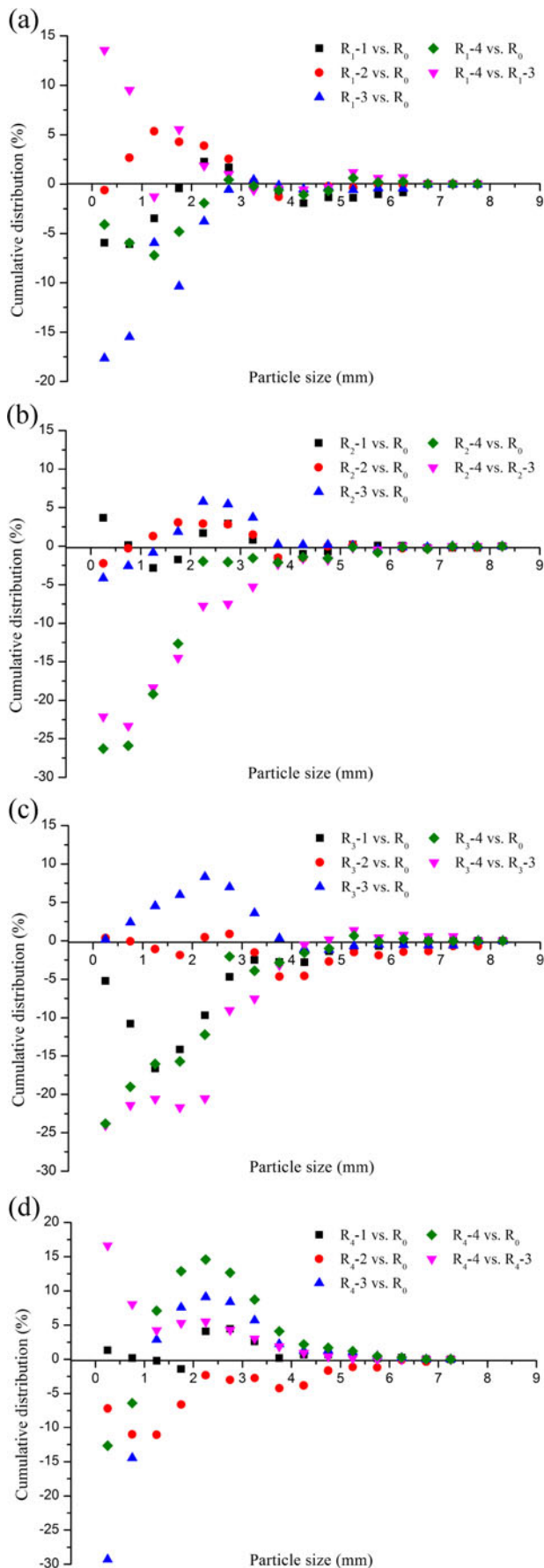
Fig. 3 Cumulative distribution of anammox granular sludge at preservation temperatures of 35 °C (a), 20 °C (b), 4 °C (c), and -30 °C (d) during the experiment

concentration in the four vials at the end of period B decreased in the order $R_3 > R_2 > R_4 > R_1$.

Granule diameter and sludge settling properties

Figure 3 shows the cumulative distributions of the granules under different storage temperatures during periods B and C. After 14 days of storage at 35 °C (79 days), the cumulative distribution of granule diameters between 2.25 and 3.25 mm was increased by approximately 0.08–2.26 %. In addition, for granule diameters larger than 3.25 mm, the corresponding cumulative distribution was reduced by approximately 0.86–1.93 % (Fig. 3a). These results illustrate that the granules were separated under a storage temperature of 35 °C. For granule diameters less than 2.25 mm, the cumulative distribution decreased by approximately 0.44–6.10 %, which is mainly because of the anammox biomass decay, as noted above (Fig. 1a). After 28 days of storage at 35 °C (93 days), the cumulative distribution of granule diameters between 0.75 and 3.25 mm was increased. In addition, the cumulative distribution of granule diameters >3.25 mm was also reduced (Fig. 3a), and the cumulative distribution of granule diameters <0.75 mm was decreased by approximately 0.61 %. These results indicate that the granule breakage and biomass decay continued and co-occurred. By the end of period B (106 days), the granule breakage and biomass decay had progressed further, and similar phenomena were observed at the storage temperatures 20, 4, and -30 °C (Fig. 3). The degree of change in the granule diameter increased in the order of $R_1 > R_4 > R_3 > R_2$, which was closely related to the storage temperature and corresponding biomass decay rate. Therefore, the preservation temperature has a significant effect on the granule diameter.

During period C, the cumulative distribution in R₁, which had a storage temperature of 35 °C, was increased for granule diameters larger than 5.25 mm. However, the cumulative distribution of granule diameters between 2.75 and 5.25 mm was decreased, which was inconsistent with the changes during period B. The cumulative distribution of granule diameters less than 2.75 mm was increased by approximately 1.0–13.6 %. These results illustrate that the granule diameter recovered gradually. For R₄, the cumulative distribution of the granule diameter increased overall, whereas for R₂, the cumulative distribution was nearly reduced overall, which may have been caused by the larger amount of nitrogen gas production leading to high values of SS_{eff} as shown in Table S1. For R₃, the cumulative distribution of granule diameters larger than 4.75 mm was increased by approximately 0.17–1.36 %, suggesting that the diameter also recovered with a continuous supply of substrates. Moreover, the cumulative distribution of



granule diameters less than 4.75 mm decreased by approximately 0.5–24.0 %. These results indicate that the preservation temperature of 20 °C (R_2) and 4 °C (R_3) promoted greater effluence compared with that of R_1 (35 °C) and R_4 (−30 °C) after the same preservation time (42 days) and HRT (3.0 h) during the 22-day reactivation period. Thus, a longer HRT should be applied to reduce the loss of anammox biomass via effluent in practical applications.

Compared with the settling velocity during the initial stage of period B, the settling velocities of the granules in R_1 , R_2 , R_3 , and R_4 decreased by different degrees, and the reduction for R_4 was larger than that of the other vials (Table 3). Moreover, an increasing number of floating granules were observed after storage for approximately 14 days at −30 °C (R_4). The upward floating velocity of floating granules was approximately $66.34 \pm 39.06 \text{ m h}^{-1}$, and the corresponding volume percentage of the floating granules in R_4 increased gradually over the storage period (Fig. S2). During the subsequent reactivation period, the settling velocities in R_1 , R_2 , and R_4 were increased, whereas that in R_3 did not increase because of the large amount of EPS in R_3 during period C. However, the volume percentage of floating granules in R_4 was approximately 50 % during the reactivation period as shown in Fig. S2. Preservation at a freezing temperature of −30 °C is difficult in practice and requires considerable energy, whereas granules stored at 20 °C achieve excellent settleability after reactivation ($R_2 > R_1 > R_4 > R_3$); thus, the improved settleability in R_2 may be one of the inherent causes for the relatively good nitrogen removal performance.

EPS

The EPS composition for these bacterial cultures was studied to investigate the EPS production and degradation behavior of the anammox consortium at different preservation temperatures. The results are shown in Table 2 and Fig. 4. The results indicated that bound EPS was the major component of the EPS (versus the soluble EPS), and the final EPS results were dependent on the bound EPS results (Table 2). The protein (PN) and polysaccharide (PS) contents of the annex granules in the total EPS increased in all vials after 6 weeks of storage. However, the increase in EPS decreased the permeability of the anammox granules, which promoted decreased settling velocities of the granules in R_1 , R_2 , R_3 , and R_4 . A similar phenomenon occurred in R_3 during the subsequent reactivation period. In this study, the settling velocities of R_1 – R_4 were consistent with the EPS content throughout the entire experiment. Therefore, the total EPS can be used to indicate the settling velocities of the anammox consortium during periods B and C. Additionally, the EPS in R_1 , R_2 , and R_4 decreased rapidly, which was mainly because the sludge with poor settling properties was washed out.

Table 3 Settling properties of anammox granules in R₁–R₄ during the experiment

Time (day)	Settling velocity (m h ⁻¹)	R ₁ (35 °C)	R ₂ (20 °C)	R ₃ (4 °C)	R ₄ (–30 °C)
65	Maximum	208.4			
	Minimum	30.46			
	Mean ± SD	65.12 ± 25.14 (81) ^a			
79	Maximum	110.4	105.5	97.65	135.4
	Minimum	27.80	28.26	31.48	10.27
	Mean ± SD	59.39 ± 16.66 (49)	62.45 ± 16.16 (75)	60.84 ± 15.44 (72)	52.40 ± 22.04 (77)
93	Maximum	106.7	129.7	199.8	71.80
	Minimum	31.61	29.17	35.58	18.75
	Mean ± SD	63.52 ± 17.71 (49)	63.21 ± 20.05 (61)	81.74 ± 30.26 (45)	39.74 ± 16.25 (13)
106	Maximum	94.27	105.5	112.0	110.1
	Minimum	37.68	28.71	20.58	37.78
	Mean ± SD	65.19 ± 14.34 (49)	62.72 ± 18.13 (54)	61.50 ± 21.13 (52)	61.29 ± 17.34 (39)
129	Maximum	107.0	109.2	90.71	102.8
	Minimum	39.38	35.99	29.44	41.44
	Mean ± SD	71.14 ± 19.97 (25)	73.76 ± 22.59 (34)	59.87 ± 15.15 (26)	67.12 ± 16.91 (43)

^a Values between brackets represent the number of granular sludge tested

However, the reasons for the increased EPS content in R₃ must be investigated in a future study.

The protein to polysaccharide (PN/PS) ratios were reduced during period B at the storage temperatures 35 and 20 °C, and the corresponding settling velocities decreased, which was mainly because of the degradation of anammox granules. Moreover, variations in the PN/PS ratios in vials C and D were complicated and exhibited a similar trend. The PN/PS ratios in vials C and D increased from their initial value of 4.22 ± 0.75 to 4.73 ± 0.24 and 4.69 ± 0.62, respectively, after 2 weeks of storage, and the corresponding PN/PS ratios decreased to 3.86 ± 0.60 and 4.15 ± 0.24, respectively, at the end of period B (on 106 days). Based on the above results, the PN/PS ratio of the

EPS is not a suitable indicator of the settleability of anammox granules during the storage period.

Morphology of the granular sludge

To monitor changes in the morphology and structure of the granular sludge, the anammox granules were studied at the beginning and end of the storage period and at the end of the reactivation period via SEM and TEM (Figs. 5 and 6). As shown in Fig. 5a, the majority of spherical and elliptical bacteria were surrounded by EPS and bacillus or filamentous bacteria. To protect microbes in harsh environments from impairment, large amounts of EPS were excreted in the four vials as shown above (Figs. 4 and 5b). After the substrate supply was recovered, the EPS contents were reduced and the surrounding cells observed as shown in Fig. 5c. However, honeycomb structures emerged in the anammox granules in R₁ and R₂, particularly in R₁, as shown in Fig. 5c, which suggests that more anammox bacteria were dissolved in R₁ than in R₂ during the preservation period. For R₃, the anammox bacteria were observed in clusters after 21 days of reactivation, whereas in R₄, several random anammox cells were distributed throughout the anammox granules with a large surplus of EPS.

The TEM analysis performed on the enriched anammox granules collected from R₀ at the end of the start-up period revealed that the dominant cells in both enrichments displayed typical ultrastructural features of anammox bacteria (Fig. 6a). After 42 days of preservation, the volume of anammox cells in R₁–R₄ was reduced compared with the volume in R₀ (Fig. 6b). A large number of the anammox cells in R₁–R₄ exhibited an irregular shape, with a number of wrinkled areas formed on

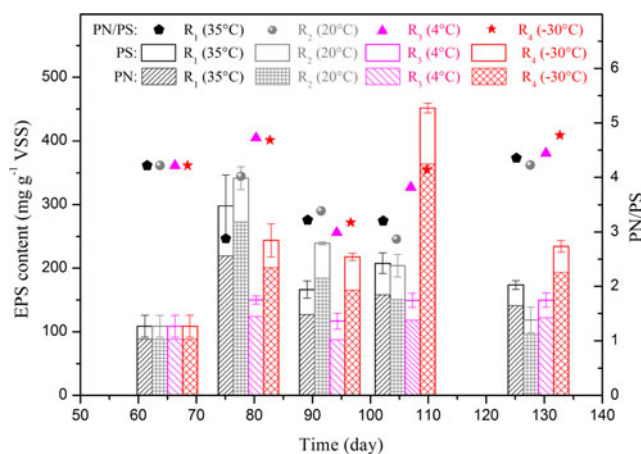


Fig. 4 Variations in the amount and composition of the EPS during the storage and reactivation periods

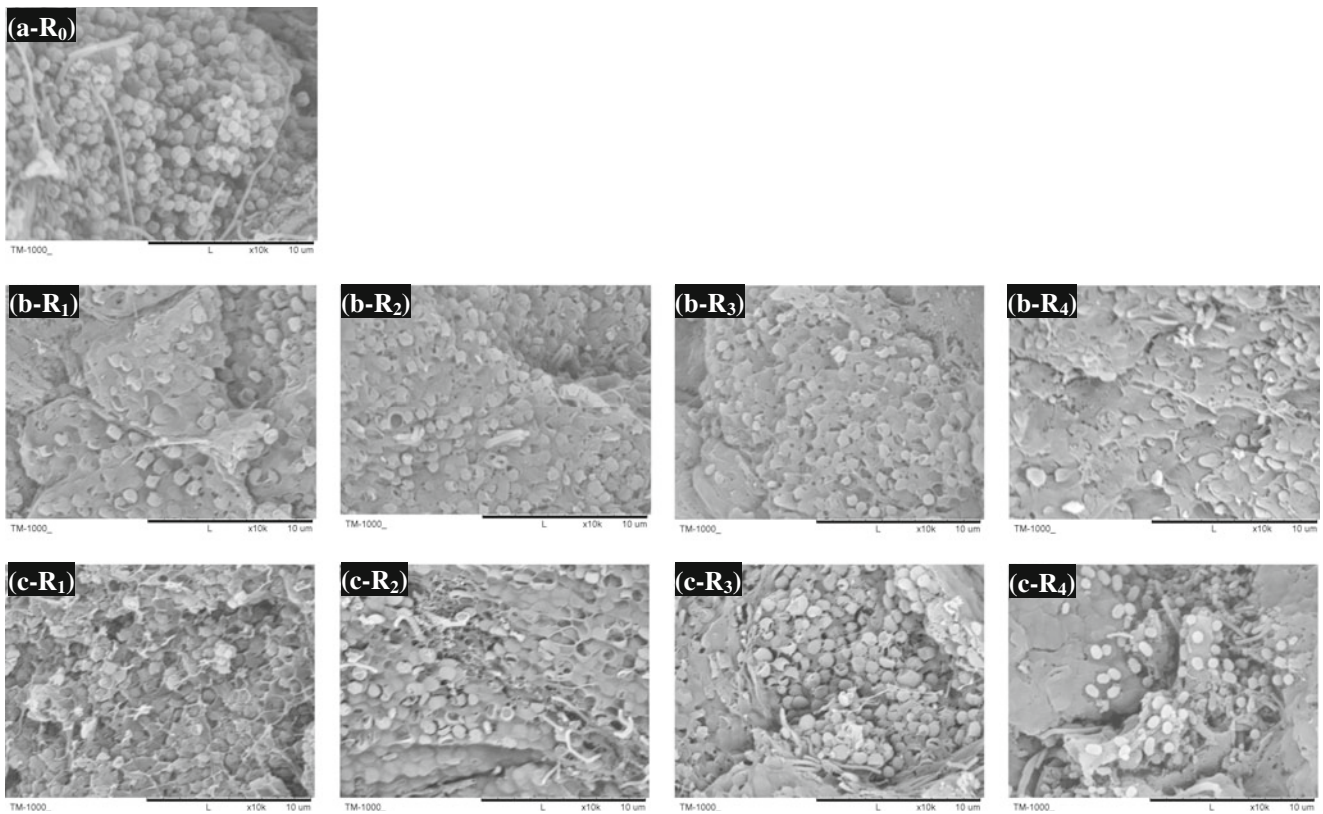


Fig. 5 SEM images of the cross-sectional morphology of anammox granules from R₁-R₄ samples collected 1 day before preservation (a), 42 days after preservation (b), and after 21 days of reactivation (c)

the anammoxosome edge, whereas the anammox cells in R₀, which had an adequate substrate, supply exhibited relatively

regular shapes. In R₁-R₄, because of the irregular shape of the anammox cells, the surface area of the anammox bacteria cells

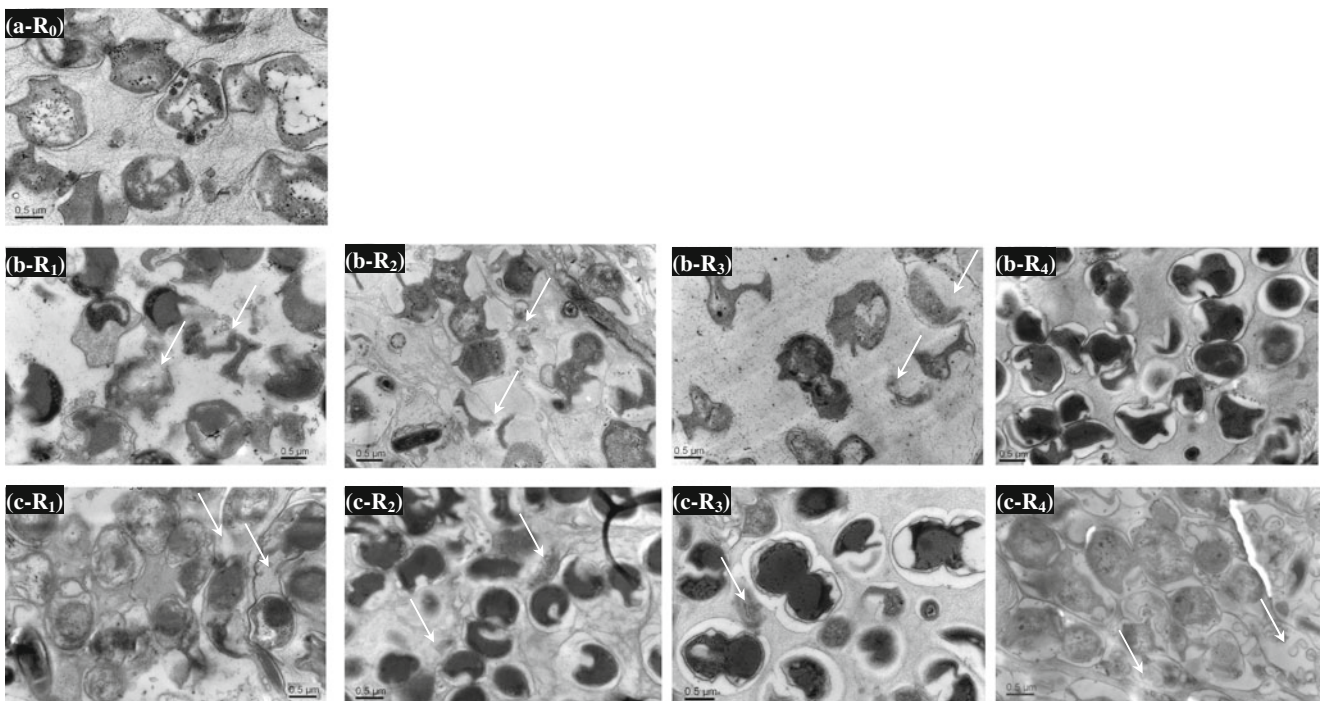


Fig. 6 TEM images of the anammox granules from the R₁-R₄ samples collected 1 day prior to preservation (a), 42 days after preservation (b), and after 21 days of reactivation (c) (bar=0.5 μm)

was increased and the substrate transfer rate was enhanced under the storage conditions. However, after 42 days of preservation, cell degradation was considerable, particularly in R_1 , R_2 , and R_3 , and the degree of degradation decreased in the order of $R_1 > R_2 > R_3 > R_4$ (Fig. 6b), which is consistent with the biomass decay rates of R_1 – R_4 . However, the anammox cells in R_3 were further degraded during the subsequent reactivation period as shown in Fig. 6c. The structures of anammox bacteria cells in R_3 were almost completely recovered after 21 days of reactivation, and these results are consistent with the phenomenon observed in the cross-sectional SEM images shown in Fig. 5c. In addition, the microbe bacteria changed because of changes in the anammoxosome structure (Fig. 6a, c) and alterations to the stoichiometric ratios during periods A and C.

Elemental analysis

To determine whether changes in the element composition of the anammox granules occurred under the preservation and reactivation conditions, the anammox granular sludges of R_0 and R_1 – R_4 , which were collected as experiment schemes, were analyzed, and the results are shown in Table S2. With respect to the theoretical values of the anammox bacteria cells, the anammox granules at the end of period A (65 days) had higher O contents and H/C, C/N, and O/C ratios and lower C, H, and N contents. After approximately 42 days of storage, the C, H, and N contents of the anammox granules all increased, whereas the O content and C/N and O/C ratios decreased. The amplitude variation of the elemental composition of the anammox granules from R_1 – R_4 increased in the order $O > C > N > H$. Bubbles were also produced in R_1 – R_4 (after 79 days) and easily observed, particularly in R_1 , R_2 , and R_4 (Fig. S2), and they were related to the degree of dissolution of anammox bacteria cells in R_1 – R_4 as noted above. Therefore, the percentages of C, H, N, and O in the granular sludge changed because of the dissolution of cellular compounds into the liquid phase. After 21 days of reactivation, the shifts in elemental composition and atomic ratios within the anammox particles from the four reactors were not notable (Table S1), indicating that a long period of time was needed for recovery to the initial elemental composition.

Inoculation and recovery reactor performance during periods A and C

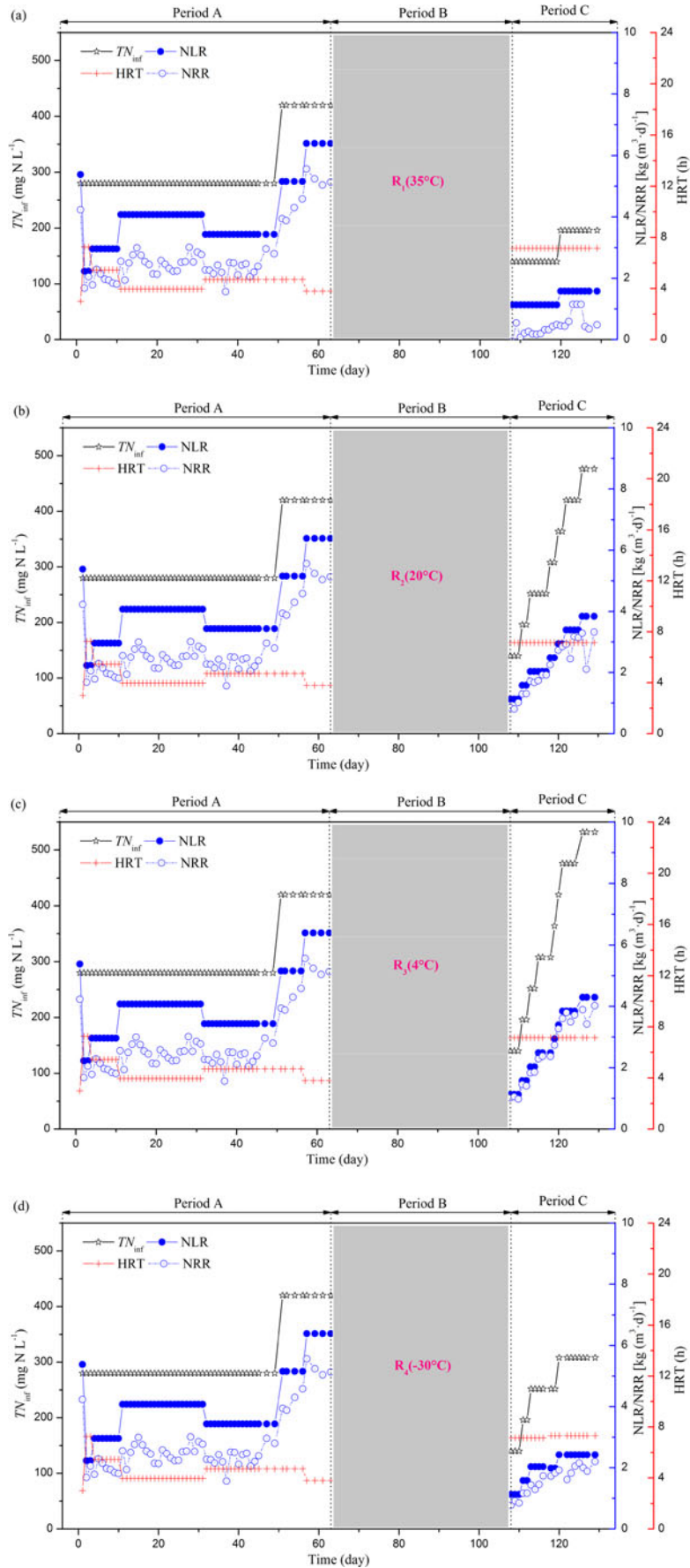
Figure 7 presents the daily changes in the TN_{inf} , HRT, NLR, and NRR of R_0 and R_1 – R_4 over the entire 129-day operation period. During period A, the parent bioreactors were gradually started up and then operated at steady-state conditions. After approximately 65 days of operation, a stable and robust anammox performance was maintained and the average NRR of R_0 was $5.24 \pm 0.23 \text{ kg N m}^{-3} \text{ day}^{-1}$, with an HRT of

Fig. 7 Nitrogen loading/removal rate, applied TN_{inf} and HRT in a UASB reactor (R_0) during the cultivation of anammox granules and the operation of R_1 (a), R_2 (b), R_3 (c), and R_4 (d)

1.58 h. During period C, the four bioreactors were recovered by feeding relatively low TN_{inf} (140 mg N L^{-1}) and HRTs of 3.0 h in the thermostatic room at $35 \pm 1 \text{ }^\circ\text{C}$. After 21 days of reactivation, the TN_{inf} of R_1 , R_2 , R_3 , and R_4 increased gradually from 140 mg L^{-1} to 196, 476, 532, and 308 mg L^{-1} , respectively, and the corresponding NRRs of R_1 – R_4 were 0.42 ± 0.06 , 2.90 ± 0.69 , 3.78 ± 0.31 , and $2.03 \pm 0.16 \text{ kg N m}^{-3} \text{ day}^{-1}$, respectively (Fig. 7). These results indicate that the reactivated capabilities increased in the order $R_3 > R_2 > R_4 > R_1$. Moreover, the modified Stover-Kincannon model was appropriate for describing R_2 , R_3 , and R_4 and produced high correlation coefficients (0.9131, 0.9959, and 0.8679, respectively). R_1 produced an irregular cellular structure and a faint anammox reaction. According to the kinetic analysis results using the modified Stover-Kincannon model, the maximum substrate utilization rate (U_{max}) of R_2 , R_3 , and R_4 was 19.50, 169.50, and $9.25 \text{ kg m}^{-3} \text{ day}^{-1}$, respectively (Fig. S3). Moreover, the nitrogen removal potential increased in the order $R_3 > R_2 > R_4 > R_1$, which is consistent with the NRRs noted above. In addition, the experimental values for the reaction ratios of nitrite to ammonium (R_S) and nitrate to ammonium (R_P) throughout the entire working stage of the reactor are shown in Table 1. The reaction ratios of R_2 , R_3 , and R_4 were all close to the reported values, whereas that of R_1 was considerably higher. These results indicate that other bacteria were dominant in R_1 , whereas the anammox bacteria was the dominant population in R_2 , R_3 , and R_4 .

Discussion

The longer required start-up period is still the main challenge preventing the practical application of anammox-based treatment processes at full scale (Ali and Okabe 2015). Preservation of the anammox biomass could be one of possible solutions to securing a sufficient seeding biomass and achieving the rapid and stable start-up of the anammox process. Several studies have been published regarding the long-term storage of various types of anammox sludge under different preservation temperatures (Ali et al. 2014; Heylen et al. 2012; Ji and Jin 2014; Vlaeminck et al. 2007; Wu et al. 2015; Zhang et al. 2015). Zhang et al. (2015) reported that the b_{AN} of anammox granules was 0.0062 day^{-1} based on decreasing VSS levels during a 30-day period of anaerobic starvation, and this value is lower than the value that was obtained here at the same starvation temperature ($35 \text{ }^\circ\text{C}$) using the same determination method. This discrepancy may have been caused by several factors, such as the starvation time, storage anammox granular sludge, and preservation liquid. Moreover, the decay rate



decreased with decreases in the storage temperature. Under ambient and mesophilic storage temperatures, the biomass decay rate was higher than that of the SAA under the long-term preservation temperature without the application of substrates. However, the SAA decay rate was larger than the biomass decay rate under the freezing temperature, which may have been caused by higher temperature promoting substrate transport rates and heterotrophic bacteria growth rates when dissolved anammox bacteria cells are used as an organic substrate. Under short-term substrate deficits, maintaining the SAA should be a top priority. The potential nitrogen removal rate and biomass retention can be used as the main performance criteria when selecting preservation conditions for storage processes, especially for the long-term preservation of anammox bacteria.

This study systematically investigated the evolution of anammox granule properties and their subsequent recovery performance after long-term storage under different preservation temperatures. Appropriate preservation methods should be identified to protect the morphological and structural characteristics of the anammox bacteria and their subsequent reactivation performance as much as possible. The results demonstrated that 4 °C was the best preservation temperature for maintaining the biomass, activity, settleability, and integrity of the anammox granules and the cellular structure of the anammox bacteria. The PN/PS ratio and heme *c* content could not effectively indicate changes in the settleability and activity of the anammox granules, respectively, and the loss of bioactivity was positively correlated with the degree of anammox bacteria cell lysis. After 42 days of storage, the performance of R₁, R₂, R₃, and R₄ and the particle characteristics from the activity recovery test revealed the advantages and disadvantages of the different preservation temperatures. During the preservation period, the anammox granules preserved at 4 °C (R₃) exhibited a better recovery performance than those preserved at 20 °C (R₂), –30 °C (R₄), and 35 °C (R₁). The comprehensive comparison indicated that 4 °C was the optimal storage temperature in terms of property maintenance and recovery performance of the anammox granular sludge. Additionally, the preservation temperatures can be ranked in the following order: 4 °C > 20 °C > –30 °C > 35 °C. This outcome is consistent with the research of Vlaeminck et al. (2007), who determined that the optimal storage temperature for the long-term storage of OLAND biofilm biomass was 4 °C.

The T_{HL} of anammox granules was longer than that of flocculent sludge under the same preservation temperature, which may have been caused by the accumulation of EPS. Heylen et al. (2012) found that storage at 4 °C was not suitable for single-cell cultures of “*Candidatus* Kuenenia stuttgartiensis” and the marine anammox species “*Candidatus* Scalindua” sp. because the cells lysed within days, which may have been related to the lack of the protective polymeric matrix present in aggregated cultures. Ji and Jin (2014) found that

the preservation temperature (4 and –40 °C) has a relatively small impact on the recovery activity of anammox granules and recommended storage at 4 °C without cryoprotectant. However, lyophilization and cryopreservation may be impracticable at a mass scale because of the complex procedures and expensive chemicals required (Ali and Okabe 2015).

Acknowledgments The authors wish to thank the Natural Science Foundation of China (Nos. 51278162 and 51578204) for the support of this study.

Compliance with Ethical Standards

Funding This study was funded by the Natural Science Foundation of China (Nos. 51278162 and 51578204).

Conflict of interest The corresponding author on behalf of all authors of the paper declares no conflict of interest.

Ethical approval This article does not contain any studies with human participants or animals performed by any of the authors.

References

- Ali M, Okabe S (2015) Anammox-based technologies for nitrogen removal: advances in process start-up and remaining issues. *Chemosphere* 141:144–153
- Ali M, Oshiki M, Okabe S (2014) Simple, rapid and effective preservation and reactivation of an anaerobic ammonium oxidizing bacterium “*Candidatus* Brocadia sinica”. *Water Res* 57:215–222
- APHA (2005) Standard methods for the examination of water and wastewater, 21st edn. American Public Health Association, Washington, DC
- Berry EA, Trumppower BL (1987) Simultaneous determination of hemes *a*, *b*, and *c* from pyridine hemochrome spectra. *Anal Biochem* 161: 1–15
- Ding S, Zheng P, Lu H, Chen J, Mahmood Q, Abbas G (2013) Ecological characteristics of anaerobic ammonia oxidizing bacteria. *Appl Microbiol Biotechnol* 97:1841–1849
- Heylen K, Ettwig K, Hu ZY, Jetten M, Kartal B (2012) Rapid and simple cryopreservation of anaerobic ammonium-oxidizing bacteria. *Appl Environ Microbiol* 78:3010–3013
- Ji YX, Jin RC (2014) Effect of different preservation conditions on the reactivation performance of anammox sludge. *Sep Purif Technol* 133:32–39
- Jin RC, Yang GF, Yu JJ, Zheng P (2012) The inhibition of the Anammox process: a review. *Chem Eng J* 197:67–79
- Jin RC, Ma C, Yu JJ (2013a) Performance of an Anammox UASB reactor at high load and low ambient temperature. *Chem Eng J* 232:17–25
- Jin RC, Xing BS, Yu JJ, Qin TY, Chen SX (2013b) The importance of the substrate ratio in the operation of the Anammox process in upflow biofilter. *Ecol Eng* 53:130–137
- Jin RC, Yang GF, Zhang QQ, Ma C, Yu JJ, Xing BS (2013c) The effect of sulfide inhibition on the ANAMMOX process. *Water Res* 47:1459–1469
- Kartal B, Kuenen JG, van Loosdrecht MCM (2010) Sewage Treatment with Anammox. *Science* 328:702–703

- Lackner S, Gilbert EM, Vlaeminck SE, Joss A, Horn H, van Loosdrecht MCM (2014) Full-scale partial nitrification/anammox experiences—an application survey. *Water Res* 55:292–303
- Leitão RC, van Haandel AC, Zeeman G, Lettinga G (2006) The effects of operational and environmental variations on anaerobic wastewater treatment systems: a review. *Bioresour Technol* 97:1105–1118
- Lotti T, Kleerebezem R, Abelleira J, Abbas B, van Loosdrecht MCM (2015) Faster through training: the anammox case. *Water Res* 81: 261–268
- Ma C, Jin RC, Yang GF, Yu JJ, Xing BS, Zhang QQ (2012) Impacts of transient salinity shock loads on Anammox process performance. *Bioresour Technol* 112:124–130
- Rothrock MJ, Vanotti MB, Szögi AA, Gonzalez MCG, Fujii T (2011) Long-term preservation of anammox bacteria. *Appl Microbiol Biotechnol* 92:147–157
- Scaglione D, Caffaz S, Bettazzi E, Lubello C (2009) Experimental determination of Anammox decay coefficient. *J Chem Technol Biotechnol* 84:1250–1254
- Strous M, Heijnen JJ, Kuenen JG, Jetten MSM (1998) The sequencing batch reactor as a powerful tool for the study of slowly growing anaerobic ammonium-oxidizing microorganisms. *Appl Microbiol Biotechnol* 50:589–596
- van der Star WRL, Abma WR, Blommers D, Mulder J, Tokutomi T, Strous M, Picioreanu C, van Loosdrecht MCM (2007) Startup of reactors for anoxic ammonium oxidation: experiences from the first full-scale anammox reactor in Rotterdam. *Water Res* 41:4149–4163
- Vlaeminck SE, Geets J, Vervaeren H, Boon N, Verstraete W (2007) Reactivation of aerobic and anaerobic ammonium oxidizers in OLAND biomass after long-term storage. *Appl Microbiol Biotechnol* 74:1376–1384
- Wett B (2006) Solved upscaling problems for implementing deammonification of rejection water. *Water Sci Technol* 53:121–128
- Wu X, Liu S, Dong G, Hou X (2015) The starvation tolerance of anammox bacteria culture at 35°C. *J Biosci Bioeng* 120:450–455
- Xing BS, Guo Q, Zhang ZZ, Zhang J, Wang HZ, Jin RC (2014) Optimization of process performance in a granule-based anaerobic ammonium oxidation (anammox) upflow anaerobic sludge blanket (UASB) reactor. *Bioresour Technol* 170:404–412
- Xing BS, Guo Q, Yang GF, Zhang ZZ, Li P, Guo LX, Jin RC (2015) The properties of anaerobic ammonium oxidation (anammox) granules: Roles of ambient temperature, salinity and calcium concentration. *Sep Purif Technol* 147:311–318
- Xu G, Zhou Y, Yang Q, Lee ZM, Gu J, Lay W, Cao Y, Liu Y (2015) The challenges of mainstream deammonification process for municipal used water treatment. *Appl Microbiol Biotechnol* 99:2485–2490
- Zhang ZZ, Buayi X, Cheng YF, Zhou YH, Wang HZ, Jin RC (2015) Anammox endogenous metabolism during long-term starvation: Impacts of intermittent and persistent modes and phosphates. *Sep Purif Technol* 151:309–317